Policy Research Working Paper 10224

Tracking Methane Emissions by Satellite

A New World Bank Database and Case Study for Irrigated Rice Production

Susmita Dasgupta
Somik V. Lall
David Wheeler

WORLD BANK GROUP
Development Economics
Development Research Group
November 2022

Policy Research Working Paper 10224

Abstract

Atmospheric methane is a potent greenhouse gas that has accounted for 23 percent of radiative forcing in the lower atmosphere since 1750. Since methane has a much shorter atmospheric duration than carbon dioxide and other greenhouse gases, it provides a critical opportunity for near-term atmospheric greenhouse gas reduction. Thus, 122 countries have joined the recently launched Global Methane Pledge to reduce methane emissions at least 30 percent from 2020 levels by 2030. Unfortunately, the Pledge confronts a serious information problem at the outset: the near-total absence of directly measured data for problem diagnosis, program design, and performance assessment. At present, priority areas for emissions reduction are identified with spatially formatted "bottom-up" emissions inventories, such as the Emissions Database for Global Atmospheric Research, which combines sectoral activity data with broadly calibrated emissions factors from engineering studies. This paper addresses the information problem by introducing a new World Bank database of monthly atmospheric methane concentrations, calculated for a high-resolution spatial grid from data provided by the European Space Agency's Sentinel-5P satellite platform. It illustrates the potential utility of the database with a global study of methane emissions from irrigated rice production, which accounts for about 10 percent of agricultural methane emissions. A comparative analysis suggests that the Sentinel-5P data supplement the Emissions Database for Global Atmospheric Research data with more fine-grained spatial information, which may support local programs to track, verify, and reward adoption of methane-reducing rice production techniques. If this approach proves valuable for irrigated rice production, it seems likely to work for other methane sources as well.

This paper is a product of the Development Research Group, Development Economics. It is part of a larger effort by the World Bank to provide open access to its research and make a contribution to development policy discussions around the world. Policy Research Working Papers are also posted on the Web at http://www.worldbank.org/prwp. The authors may be contacted at sdasgupta@worldbank.org.

Tracking Methane Emissions by Satellite: A New World Bank Database and Case Study for Irrigated Rice Production

Susmita Dasgupta*
Somik V. Lall
David Wheeler

World Bank

Keywords: CH4 emissions, Sentinel-5P, Agricultural emissions, Irrigated rice production

JEL Classification: Q01, Q54, R28, R48, R58

The research is funded by the Knowledge for Change Trust Fund, administered by the World Bank.

* Authors' names in alphabetical order. Our special thanks to Vijay Jagannathan, who inspired this project.

1. Introduction

The World Meteorological Organization forecasts that the current greenhouse gas (GHG) emissions trend will increase global temperature 3-5 degrees C by 2100 (Reuters 2018). This would far overshoot the 2-degree limit pledged by the 2015 Paris Climate Accords (COP21) and might have a catastrophic impact (Steffen et al. 2018; World Bank 2012). In response, several industrial nations pledged very steep emissions reductions at the Leaders' Summit on Climate in April 2021. The response deepened at COP26 in Glasgow with the introduction of the Global Methane Pledge, whose 122 current participating nations have joined a collective effort to reduce global methane emissions at least 30 percent from 2020 levels by 2030. The Pledge highlights the particular importance of methane reduction: "Methane is a powerful but short-lived climate pollutant that accounts for about half of the net rise in global average temperature since the pre-industrial era. Rapidly reducing methane emissions from energy, agriculture and waste … is regarded as the single most effective strategy to keep the goal of limiting warming to 1.5˚C within reach while yielding co-benefits including improving public health and agricultural productivity."[1]

Unfortunately, pledges to reduce methane and other GHGs confront a striking information problem at the outset: National reporting has relied almost entirely on voluntary disclosure of emissions calculated by "bottom-up" methods that apply engineering parameters to estimated activity levels in emissions-generating sectors. Recently, advances in satellite-based measurements have shown the potential to supplement voluntary national reporting with directly-observed, transparent measures of GHG emissions. High-resolution observations of atmospheric GHG concentrations are now available from several platforms, including NASA's OCO-2 and OCO-3 instruments, the European Space Agency's METOP-A and TROPOMI (Sentinel-5P) platforms, China's TANSAT and the Japan Space Exploration Agency's GOSAT and GOSAT-2. Detailed technical assessments of measures from these platforms have verified that they provide useful and comprehensive information for global carbon emissions analysis (Sha et al. 2021; Weir et al. 2021; Nassar et al. 2021; Pan et al. 2021; Wu et al. 2020; Hakkarainen et al. 2019; Labzovskii et al. 2019).

This paper focuses on satellite measurement to support implementation of the Global Methane Pledge. The first requirement is an easily-updated template for tracking atmospheric CH4 (methane) concentrations at local and regional scales. Using observations from the Sentinel-5P (S5P) platform of the European Space Agency (ESA), we develop the template from data filtering techniques pioneered by Hakkarainen et al. (2019) and applied to satellite-based CO2 measures by Dasgupta, Lall and Wheeler (2022a,b).

The second requirement is support for prioritizing actions to reduce methane emissions from energy, agricultural and waste subsectors whose spatial distributions are highly non-uniform across and within countries. At present, priority-setting is guided by spatially-formatted "bottom-up" estimates from national or global emissions inventories such as the Emissions Database for Global Atmospheric Research (EDGAR). These inventories combine sectoral activity

[1] https://www.globalmethanepledge.org/#about

data with broadly-calibrated emissions factors (Crippa et al. 2020; Solazzo et al. 2021). Policy analysts can use spatial inventory data to identify emissions-intensive areas, trace the emissions to specific subsectors, and perform benefit-cost assessments of alternative technologies for emissions reduction.

Satellite-based methane measurements have the potential to inform priority-setting by supplementing "bottom-up" emissions estimates with direct observations. The value added by the satellite-based approach depends on the comparative accuracy of the estimated sectoral outputs and emissions intensities used by existing inventories. This paper initiates a round of empirical assessments with a comparative study for irrigated rice production. It combines atmospheric CH4 concentrations from our Sentinel-5P database with georeferenced data on paddy areas, production yield and planting seasons from IFPRI (2019) and RiceAtlas (Laborte et al. 2017). The results are compared with agricultural CH4 emissions estimates from the EDGAR database.

The remainder of the paper is organized as follows. Section 2 describes our global methane database, and Section 3 introduces the application to irrigated rice production. Section 4 describes the computation of CH4 concentrations over irrigated rice production areas. Section 5 incorporates IFPRI and RiceAtlas data to study the relationship between the scale of irrigated rice fields and local methane concentrations, and to identify outlier areas where methane concentrations deviate significantly from scale-based expectations. Section 6 incorporates EDGAR emissions estimates and analyzes their relationship to the scale of irrigated fields. Section 7 assesses the "value added" of S5P by identifying outlier areas where S5P methane concentrations deviate significantly from expectations based on field scale and EDGAR estimates. Section 8 integrates the S5P concentration data and IFPRI production data to develop an index of local methane intensity (methane emissions per ton of rice produced). Section 9 summarizes and concludes the paper.

2. The Atmospheric Concentration of Methane

2.1 Global Warming Potential

The concentration[2] of atmospheric methane (CH4) was 1,857 ppb in 2018, about 2.6 times greater than its estimated level in 1750 (Saunois et al. 2020). The primary sources of the increase are emissions from agriculture, fossil fuel production and use, and waste disposal (Ciais et al. 2013). Atmospheric CH4 is a potent greenhouse gas, with a global warming potential 28 times the potential of CO2[3] (Myhre et al. 2013). Although current anthropogenic CH4 emissions are only 3% of anthropogenic CO2 emissions by volume, they are accountable for 23% of the radiative forcing in the lower atmosphere since 1750 (Etminan et al. 2016). CH4's average 9-year duration in the atmosphere (Prather et al. 2012) is dwarfed by the multi-century duration of CO2. By implication, rapid CH4 emissions reduction should have high priority because it can reduce

[2] Technically, the surface dry air mole fraction.
[3] This ratio is calculated for a 100-year time horizon and without considering climate feedbacks.

radiative forcing significantly within a decade (Shindell et al. 2012). To assist the stakeholder community, we have worked with the World Bank's Development Data Hub to publish an online database that makes georeferenced CH4 atmospheric concentration data more accessible to non-specialists.

2.2 Satellite Measurement Components

We have constructed the atmospheric CH4 concentration database from observations by the ESA's Sentinel-5P platform that typically number over 200,000 per day. We locate each observation in the 25-km global grid developed for CO2 analysis by Dasgupta, Lall and Wheeler (2022a,b). The dominant component in each observation is the global stock of atmospheric CH4 molecules that have accumulated during the past decade. The second component is seasonal, determined by natural processes over the annual cycle. The third component is geographic: Emitted CH4 molecules tend to remain within their latitude bands of origin for significant periods before full global mixing.

The fourth observation component is determined by local anthropogenic CH4 emissions, which remain near their point of origin long enough to be distinguished from the three "background" components. We term this the "concentration anomaly" since it measures the local deviation from the global background CH4 concentration. As previously noted, its primary sources are emissions from agriculture, fossil fuel production and use, and waste disposal.

2.3 Data Collection and Processing

The ESA's Sentinel-5P (S5P) operates in a Sun-synchronous near-polar orbit with an equatorial crossing at 13:30 local solar time. It completes 14 orbits of the Earth per day, with a site revisit time of one day and a current spatial resolution of 5.5 x 3.5 km. We use the S5P L2 Offline georeferenced measures of XCH4 (the column average dry air mixing ratio of methane[4]), corrected for bias associated with XCH4 dependence on surface albedo.[5]

Recent global research by Sha et al. (2021) has shown that S5P CH4 measures correspond very closely to independent measures taken at ground stations maintained by TCCON (Total Carbon Column Observing Network).[6] Sentinel-5P's bias-corrected XCH4 data exhibit a difference of −0.26±0.56 % when compared with the corresponding TCCON data. Per the ESA's recommendation, we use only pixels with quality values greater than 0.5. The data have been

[4] the total atmospheric column between the surface and the top of the atmosphere normalized to the corresponding dry air column.

[5] For more technical details, see the documentation at https://sentinel.esa.int/documents/247904/3541451/Sentinel-5P-Methane-Product-Readme-File

[6] Current TCCON sites are located in the United States, China, Canada, Germany, Poland, France, Japan, Australia, New Zealand, the Republic of Korea, Réunion, and Ascension Island.

downloaded from the ESA's AWS repository managed by MEEO (Meteorological Environmental Earth Observation).[7,8]

We filter the bias-corrected XCH4 data for local concentration anomalies, or differences between observed and background CH4 at each point. We calculate background CH4 using the methodology of Hakkarainen et al. (2019), which isolates local anomalies from the three background components described above. We compute the daily median XCH4 for each 10-degree latitude band and linearly interpolate the result to each S5P observation with 1-degree resolution. Following Hakkarainen, we use the median as the representative value because it is not skewed by extreme observations. We subtract this background value to compute the local anomaly for each observation. Then we compute monthly mean values of concentration anomalies for each 25-km grid cell in our database.

Figures 1 and 2 display mean annual CH4 concentration anomalies for the terrestrial globe in 2020 and 2021. Country outline maps are superposed to aid interpretation. Although there are some evident year-to-year differences, several common patterns emerge. The first is the effect of pixel quality on coverage density. In both years, exclusion of lower-quality pixels leads to coverage gaps in western China, parts of Siberia, Indonesia, Papua New Guinea, northwestern South America and western Canada. The second common pattern is the widespread incidence of large positive anomalies in continental south, southeast and east Asia; the Persian Gulf region and the North African littoral; South Sudan and southern Nigeria; southern and western Brazil (with an extension into Bolivia); south-central and north-central United States; and numerous regions in the Arctic. In counterpoint, widespread negative anomalies are evident in the western United States and Mexico; southwest China; and a region that includes Mongolia and areas to its north and northeast in China and the Russian Federation.

[7] https://www.meeo.it/

[8] The data are available in NetCDF format at the ESA's AWS repository, https://meeo-s5p.s3.amazonaws.com/OFFL/L2__CH4, with filenames catalogued at https://scihub.copernicus.eu/catalogueview/S5P/

Figure 1: Local methane concentration anomalies, 2020

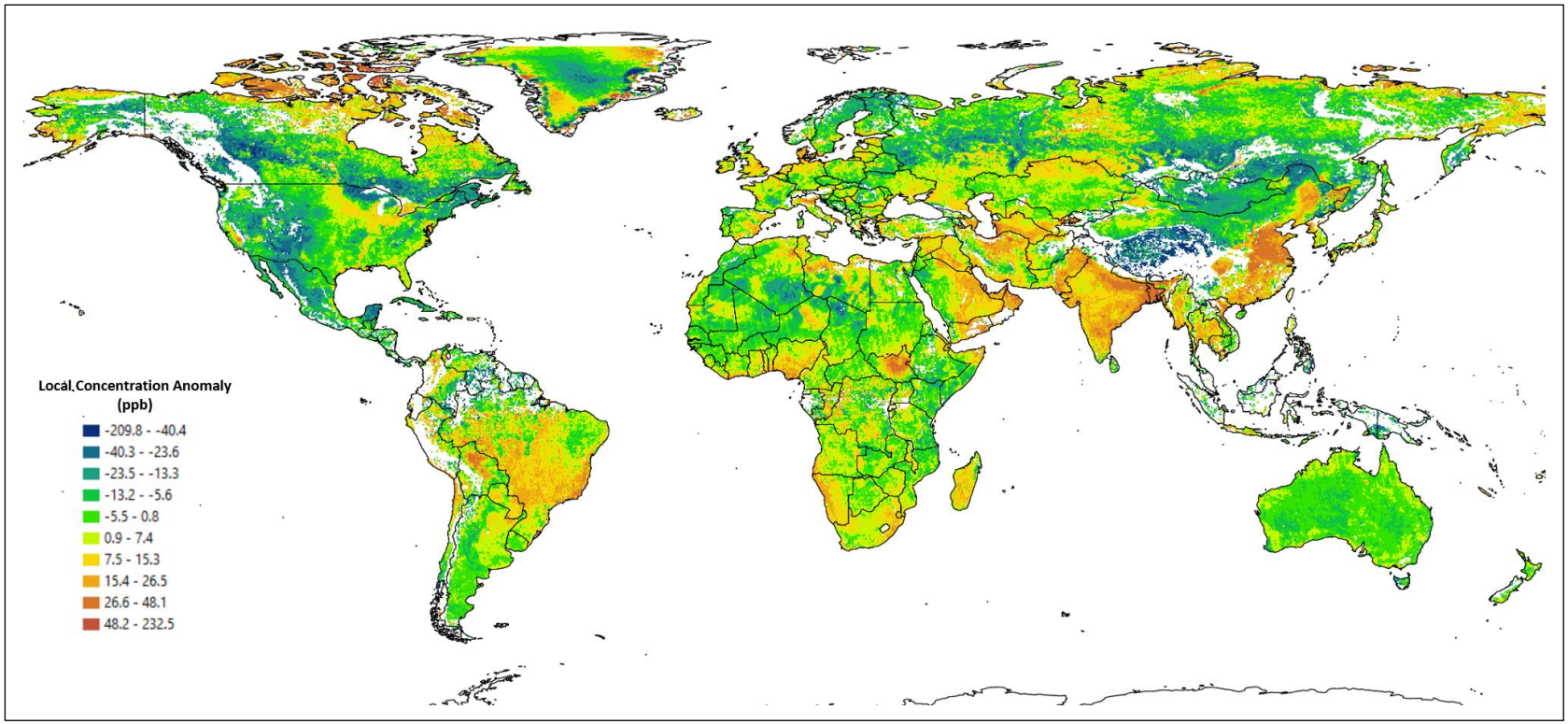

Figure 2: Local methane concentration anomalies, 2021

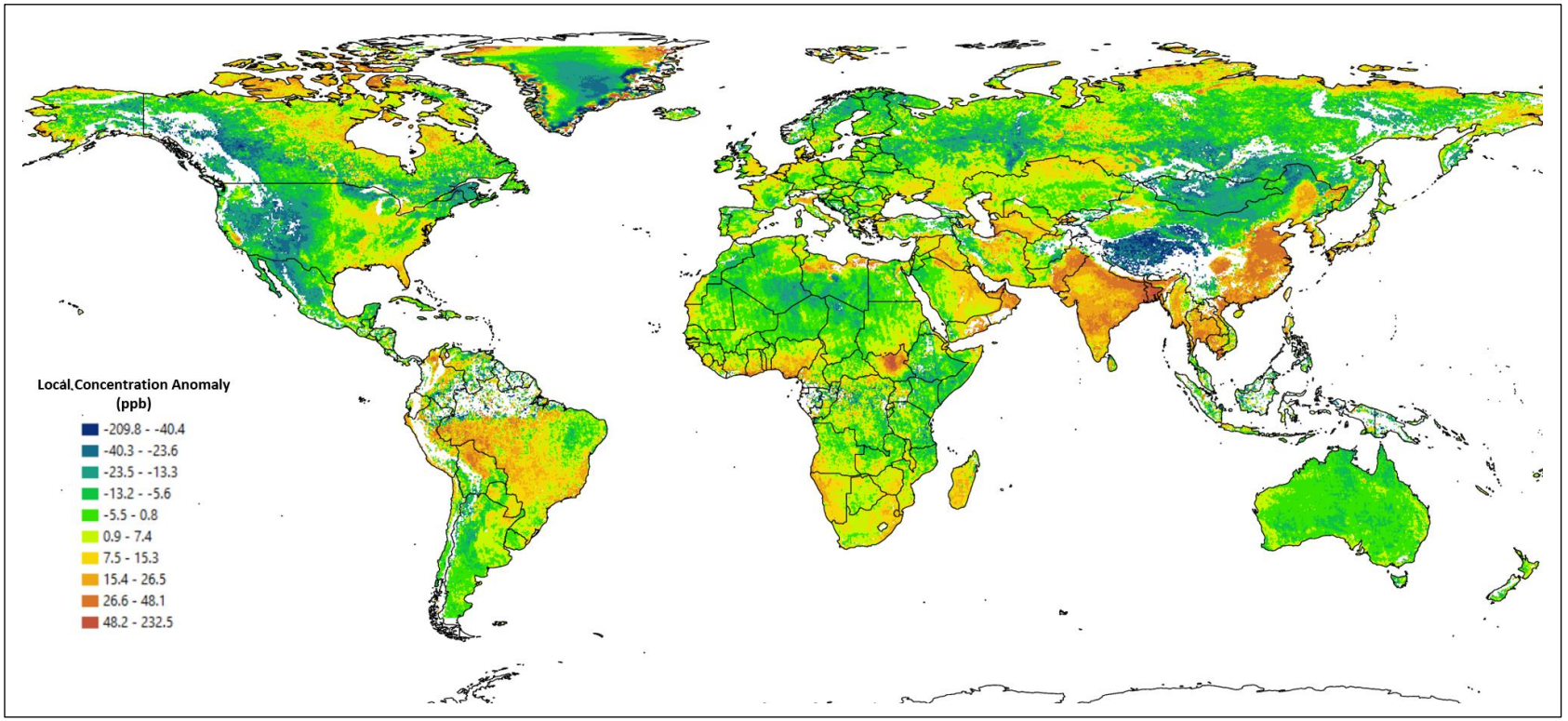

3. An Application for Irrigated Rice Production

The CH4 database has been designed to complement the CO2 database developed in Dasgupta, Lall and Wheeler (2022 a,b). Both are intended to assist global stakeholders with readily-usable, internationally-comparable and objectively-verifiable information about greenhouse gas emissions. We believe that 25-km resolution strikes a reasonable balance between robust estimation of cell means, given the available data, and the resolution required for analysis at subregional scales.

We illustrate with a global analysis of emissions from irrigated production of rice, the staple crop for the majority of the world's population (Adhya et al. 2014). In 2013, rice was harvested on 165 million hectares of land in 100 countries, with 90 percent of global production in Asia. Lowland irrigated fields occupy about 80 million hectares and produce 75 percent of the global crop (FAO 2014; Fischer et al. 2014).

Figures 3 and 4 display the global distribution of irrigated rice production by field extent and yield, respectively, estimated by a team affiliated with the International Food Policy Research Institute (IFPRI) (Yu et al. 2020). Aside from the vast irrigated areas in South, Southeast and East Asia, Figure 3 reveals smaller areas under particularly intense cultivation in the United States (California and the Mississippi River Valley), southern Brazil and Uruguay, northern Italy, The Gambia, Mali, the Nile Delta and Madagascar. Figure 4 displays a yield pattern that is somewhat different, with evident high-yield areas in the United States, southern Brazil and Uruguay, southern Spain, northern Italy, the Nile Delta, central and northeastern China, and eastern Australia. South and Southeast Asia offer the most striking contrast, with widespread cultivation intensity in Figure 3 but relatively low yields in Figure 4.

The georeferenced IFPRI data have higher spatial resolution (0.083 degrees) than our spatial grid for CH4 anomalies (0.25 degrees). To incorporate them, we map each IFPRI pixel to a grid cell. Then we add IFPRI pixel information to obtain total production and irrigated rice land in each grid cell, and divide the former by the latter to calculate the yield.

In this exercise, we use the CH4/IFPRI data to address four related questions about the irrigated rice production areas displayed in Figures 3 and 4. First, do CH4 concentration anomalies from the database align with the scale of irrigated rice production areas? Second, what is the alignment between the same area scale and EDGAR's "bottom-up" emissions estimates that combine detailed sectoral activity data with regionally-tailored emission factors? Third, what is the "value added" by the S5P CH4 data in identifying methane emissions from irrigated rice production that are not identified by area scale and EDGAR data in combination? Finally, what can the S5P data tell us about the global distribution of CH4 intensities, or methane emissions per unit of irrigated rice production? The following sections address these questions in turn.

Figure 3: Irrigated rice production, area harvested (hectares)

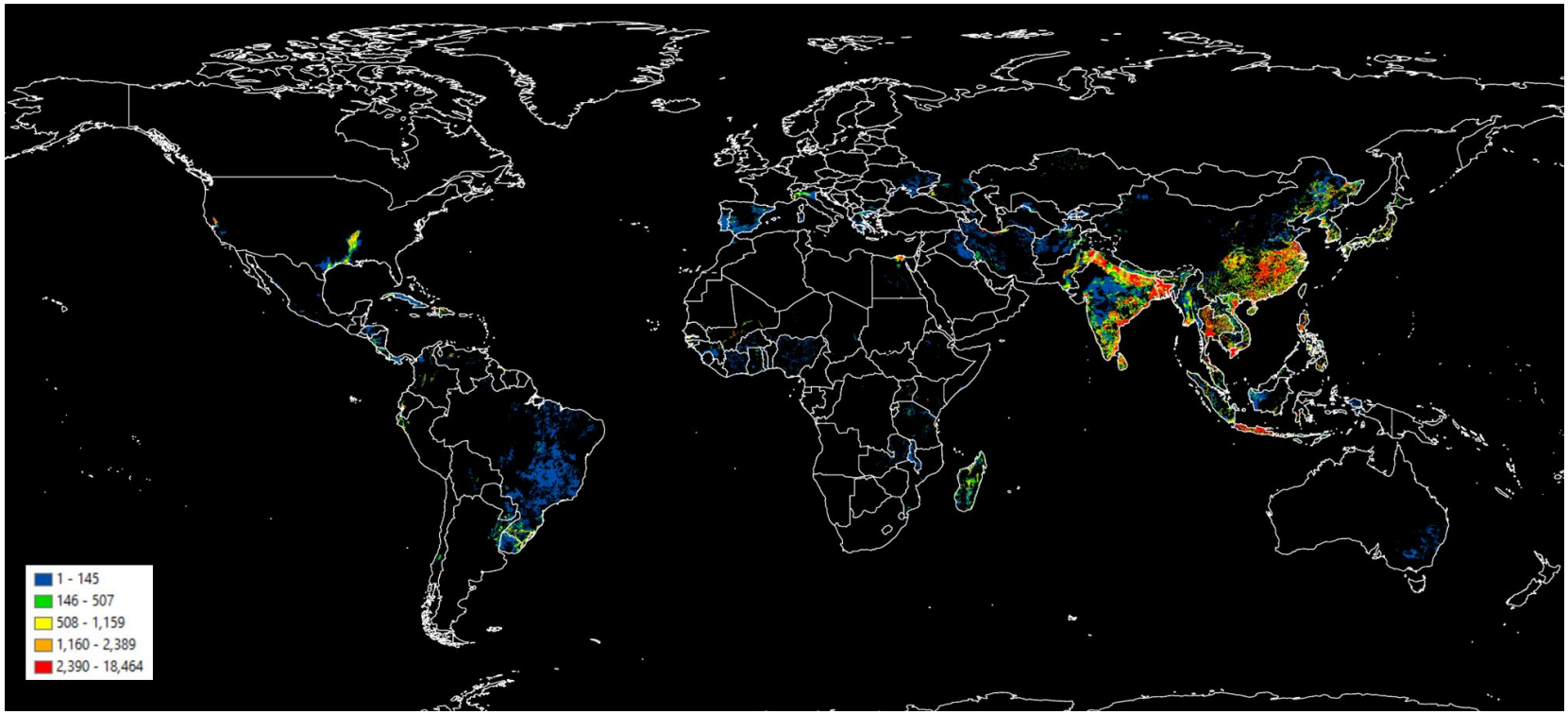

Source: IFPRI (2019)

Figure 4: Irrigated rice production, yield (kg/hectare)

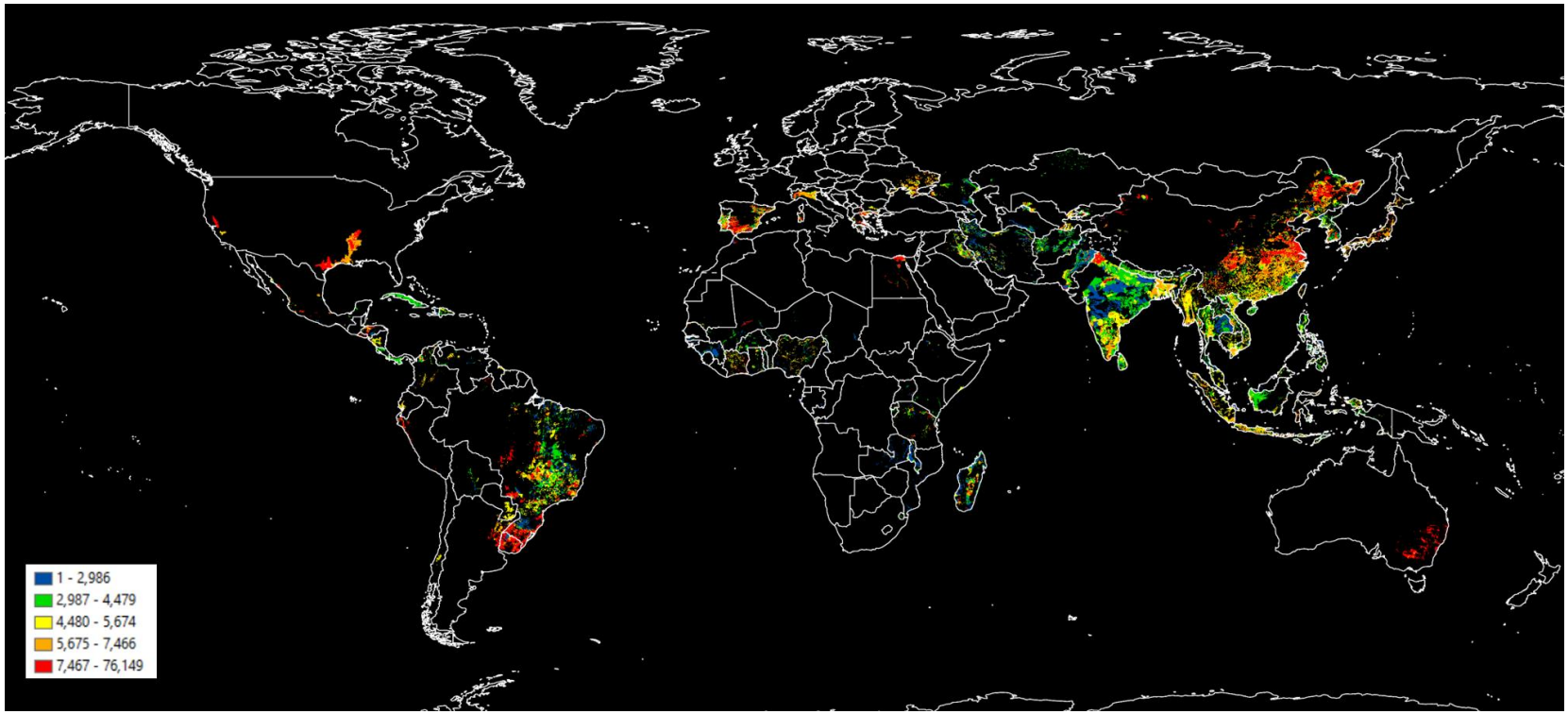

Source: IFPRI (2019)

4. CH4 Concentration Anomalies over Irrigated Rice Production Areas

The current version of our database provides monthly mean CH4 concentration anomalies in 266,884 terrestrial grid cells at 25 km resolution for 2020, 2021, and the first half of 2022. The means are calculated from daily observations that are pre-filtered to remove global background concentrations, trends, and latitudinal clustering. We overlay the IFPRI shapefile on the global grid to extract cells with irrigated rice production. For this exercise, CH4 observations in each cell are limited to the months in which fields are actually flooded. We identify those months using RiceAtlas, a spatial database of global rice calendars developed by Laborte et al. (2017). RiceAtlas distinguishes up to three rice cultivation seasons and identifies the first flooding and harvest days for each season by day-of-year.

For each pixel in RiceAtlas, we use this information to identify months that lie fully within periods lasting from first field flooding to ten days before harvest (to account for pre-harvest drainage (IRRI, 2022)). Then we intersect the RiceAtlas shapefile with our SP5/IFPRI spatial grid and assign each grid cell the cultivation calendar with the greatest representation in that cell.[9] For grid cells with IFPRI irrigated rice areas but no RiceAtlas information, we assign the cultivation calendar in the nearest RiceAtlas cell. We compute mean grid cell CH4 anomalies for all within-calendar monthly observations during the period 2020-2022.

5. Sources of Variation in Concentration Anomalies

5.1 The Effect of Field Scale

We posit a monotone increasing relationship between CH4 anomalies and the scale of IFPRI flooded fields in a grid cell and perform a linear regression using percentile values.[10] To test for robustness, we use alternative estimators that incorporate different assumptions about the structure of the stochastic error term (ε_{it}) in the model. These techniques produce the same point estimates for model parameters, but their differing estimates of standard errors (and the accompanying t-statistics) may lead to very different inferences about the statistical significance of model variables. Table 1 reports our results; we replicate the point estimates in columns (1)–(3) to aid interpretation of the t-statistics. We include standard linear regression results along with results for robust standard errors (SE), and standard errors adjusted for 1,149 clusters defined by level-1 administrative units (states, provinces, etc.) in the 99 countries in the regression database.

The results in Table 1 are all highly robust, suggesting that an increase of one percentile in the extent of IFPRI-identified irrigated rice fields is associated with a percentile increase of 0.5 in the

[9] Most grid cells have only one cultivation calendar; this assignment rule applies to grid cells that straddle two or more RiceAtlas calendars.

[10] Percentile value regressions are robust to alternative specifications of functional forms, imposing only the assumption that dependent and independent variables have a monotone increasing relationship. Rank regressions also have these characteristics.

local CH4 anomaly. Regression-predicted values and residuals are presented in Figures 5 and 6, respectively. Figure 5 displays the expected percentile values of local CH4 concentration anomalies, given the extent of irrigated rice fields, during the months of field flooding. In Asia, the areas with highest expected values are in central and eastern China, western Korea (North and South), western Thailand, northern and southern Vietnam, northern and southern Philippines, Java (Indonesia), southern Myanmar, Sri Lanka, Bangladesh, northern and eastern India and central and southern Pakistan. Other regions with particularly-high expected local CH4 anomalies include the Iranian Caspian Sea littoral, the Russian Sea of Azov littoral, the Nile Delta, and California and the Mississippi River Valley in the United States.

5.2 The Role of Agricultural Techniques

After controlling for the scale of flooded fields, we would also expect concentration anomalies to vary with the methane intensity of production techniques. Rice production in flooded fields produces methane because oxygen does not penetrate the soil when it is blocked by water. This promotes the growth of methane-producing bacteria. A variety of techniques can shorten the period of water blockage, including a single field drainage in the mid-season; alternate wetting and drying (AWD), dry seeding instead of transplanting rice into flooded fields, and "aerobic" systems that grow rice in well-drained soil (Adhya et al. 2014).

While perfect water management under ideal water supply conditions could theoretically reduce water blockage and methane emissions by 90%, actual adoption of methane-reducing techniques is strongly affected by the reliability of control over irrigation water, as well as potential variations in water coverage related to field size and degree of leveling (Adhya et al. 2014). Variation in these factors within and across regions can be expected to generate substantial differences in water blockage and methane intensity per hectare. Research on the effects of local production techniques remains limited to some areas (e.g. Nguyen et al. 2022; Devkota et al. 2019; Stuart et al. 2018). For rice production areas more generally, we would expect S5P CH4 observations to capture part of the interarea variation produced by different techniques.

5.3 Identifying Outlier Areas from Regression Residuals

Figure 6 displays residuals from the regression results reported in Table 1. They have potential interest for policy analysis because they identify areas where variations in irrigation water use and field conditions may be associated with unusually high or low CH4 anomalies, after controlling for field scale. In Asia the areas with much higher-than-expected values are in northeastern China and Western India, while areas with much lower-than-expected values are in western China, southwestern China, Hainan (China), central Vietnam, southern Thailand, southern Philippines, Sri Lanka and the entirety of Indonesia. Elsewhere, areas with higher-than-expected values include northern Italy, southern Nigeria, southeastern Brazil, central Bolivia and northern Colombia. Regions with notably lower-than-expected values include southeastern Australia, central Islamic Republic of Iran, the Nile Delta, northern Madagascar, southern Mali and eastern Guinea, northern Senegal, western Spain, Uruguay, western República Bolivariana de Venezuela, Costa Rica, Cuba, the Dominican Republic, western Mexico and California.

Table 1: Local CH4 concentration anomalies (S5P) vs. irrigated rice field extents (IFPRI)

Dependent variable: CH4 Anomaly Percentile

	OLS	Robust	Cluster
Field Extent Percentile	0.507*** (82.75)	0.507*** (84.93)	0.507*** (13.09)
Const.	24.92*** (69.94)	24.92*** (70.25)	24.92*** (11.01)
R^2	0.2574	0.2574	0.2574
Obs.	19,755	19,755	19,755

t statistics in parentheses:
* p<0.05 ** p<0.01 *** p<0.001

Figure 5: Local CH4 anomalies: Regression-predicted percentiles

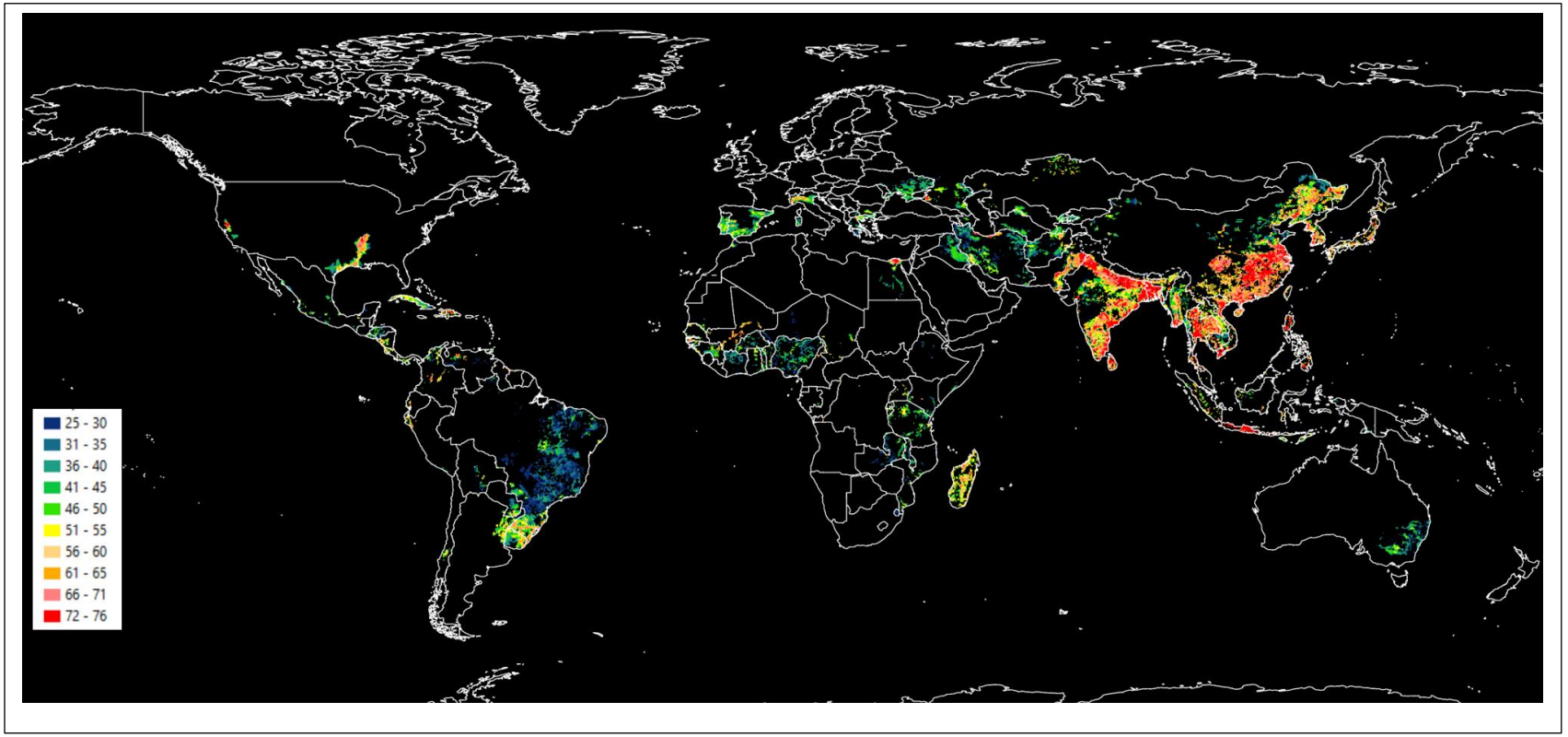

Figure 6: Local CH4 anomalies: Regression residuals

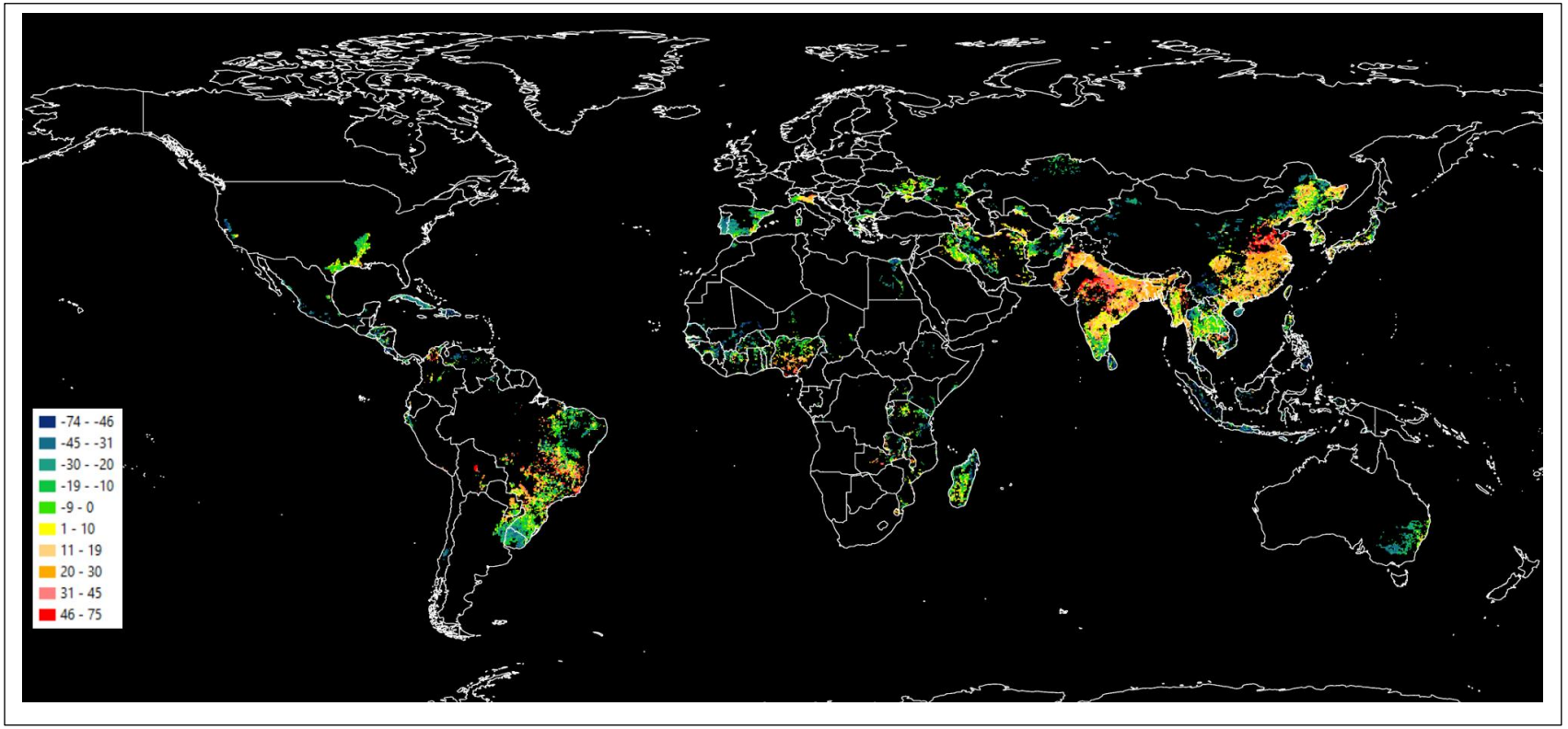

6. EDGAR Emissions versus The IFPRI Field Scale

For comparison, we introduce the latest (2018) agricultural methane emissions estimates[11] from the Emissions Database for Global Atmospheric Research (EDGAR (2022)), the global standard for "bottom-up" emissions estimation that combines detailed sectoral activity data with emissions factors that are adjusted for broad regional differences that may incorporate differences in water supply conditions and field configurations.

Since sectoral activity data drive the EDGAR emissions estimates, we could expect them to exhibit a relatively close relationship. Table 2 presents OLS, Robust and Cluster results for a percentile regression model that relates EDGAR emissions to the IFPRI estimates of irrigated rice field extent. The fit is excellent; the regression R^2 is 0.5856, as compared with 0.2574 for the SP5 CH4 anomalies in Table 1.

Table 2: EDGAR CH4 emissions estimates vs. irrigated rice field scale (IFPRI)

Dependent variable: EDGAR Emissions Percentile

	OLS	Robust	Cluster
Field Extent Percentile	0.771*** (167.06)	0.771*** (182.20)	0.771*** (31.57)
Const.	11.46*** (42.70)	11.46*** (43.17)	11.46*** (7.84)
R^2	0.5856	0.5856	0.5856
Obs.	19,755	19,755	19,755

t statistics in parentheses:
* p<0.05 ** p<0.01 *** p<0.001

Although the regression R^2 is relatively high, substantial unexplained variance remains because EDGAR's regional adjustments prevent a near-perfect global fit between the EDGAR estimates and field scale alone. The EDGAR regional adjustments are intended to capture the broad effects of typical regional differences in water use and field configuration that affect methane emissions, given field scale. For the current exercise, a critical question follows: Do the SP5 CH4 measures

[11] Available online at https://cidportal.jrc.ec.europa.eu/ftp/jrc-opendata/EDGAR/datasets/v60_GHG/N2O/AGS/v6.0_N2O_2018_AGS.0.1x0.1.zip

identify spatial variations in methane emissions that are not already captured by the IFPRI and EDGAR data?

7. S5P CH4 Value Added

We assess the "value added" of SP5 CH4 measures in a two-step exercise. First, we regress those measures on IFPRI field extents and EDGAR CH4 emissions. Table 3 shows that both variables contribute significantly to explaining SP5 CH4 variations. The regression residuals are the "value added" of S5P – the component of spatial variation in methane emissions not explained by field extents or EDGAR emissions.[12]

Table 3: Determinants of local SP5 CH4 anomalies

Dependent variable: CH4 Anomaly Percentile

	OLS	Robust	Cluster
Field Extent Percentile	0.199*** (21.92)	0.199*** (21.24)	0.199*** (4.96)
EDGAR Emissions Percentile	0.400*** (44.36)	0.400*** (44.94)	0.400*** (10.74)
Const.	20.34*** (57.28)	20.34*** (58.31)	20.34*** (8.61)
R^2	0.3247	0.3247	0.3247
Obs.	19,755	19,755	19,755

t statistics in parentheses:
* p<0.05 ** p<0.01 *** p<0.001

Figure 7 displays the global distribution of the value-added component. Large positive outliers (colored light and dark red) denote areas where S5P CH4 anomalies are much higher than would be predicted with knowledge of field extents and EDGAR emissions alone. The converse is true for large negative outliers.

[12] It may also be useful to interpret this as a three-step process. The first step performs separate regressions of S5P CH4 anomalies and EDGAR emissions on IFPRI field extents. The second step computes residuals for both regressions. The third step regresses the S5P residuals on the EDGAR residuals and computes the residuals from that exercise. These residuals incorporate the S5P CH4 anomalies that are not explained by EDGAR residuals, after both variables have been purged of field scale effects.

Among positive outliers, the most easily-identifiable clusters are in west-central India and northeastern China. Smaller clusters are visible in western Zambia, southern Nigeria, southeastern Brazil, central Bolivia and northern Colombia. Negative outlier clusters are visible in southeastern Australia, Indonesia, southern Philippines, southern Thailand, central Vietnam, southwestern and far western China, Sri Lanka, central Islamic Republic of Iran, the Nile Delta, northeastern Tanzania, northern Madagascar, central and southern Mali, western Spain, Uruguay, Cuba, the Dominican Republic, western República Bolivariana de Venezuela, the western coastal areas of Central America and Mexico, and California.

Table 4 provides a summary view, aggregated by states and provinces for administrative units that have more than 10 observations (GADM 2022). The table displays top-20 outliers in descending order. Among the countries with positive outliers, India is represented by 6 areas; five countries have 2 areas (China, Myanmar, Nigeria, Brazil, Bolivia); and four countries have 1 (Azerbaijan, Pakistan, Paraguay, Italy). Among countries with negative outliers, Indonesia has 7 areas; four countries have 2 areas (Mali, Portugal, Cuba, Uruguay); and five countries have 1 (China, Japan, the Arab Republic of Egypt, Guinea, the República Bolivariana de Venezuela). In summary, India and Indonesia dominate the extreme outlier countries at opposite ends of the outlier distribution and, with the exception of China, countries have states/provinces clustered by positive or negative status. Of course, this is not true for the entire set of states/provinces, which number in the hundreds. Full results are available from the authors on request.

Figure 7: Value-added component of S5P CH4 anomalies

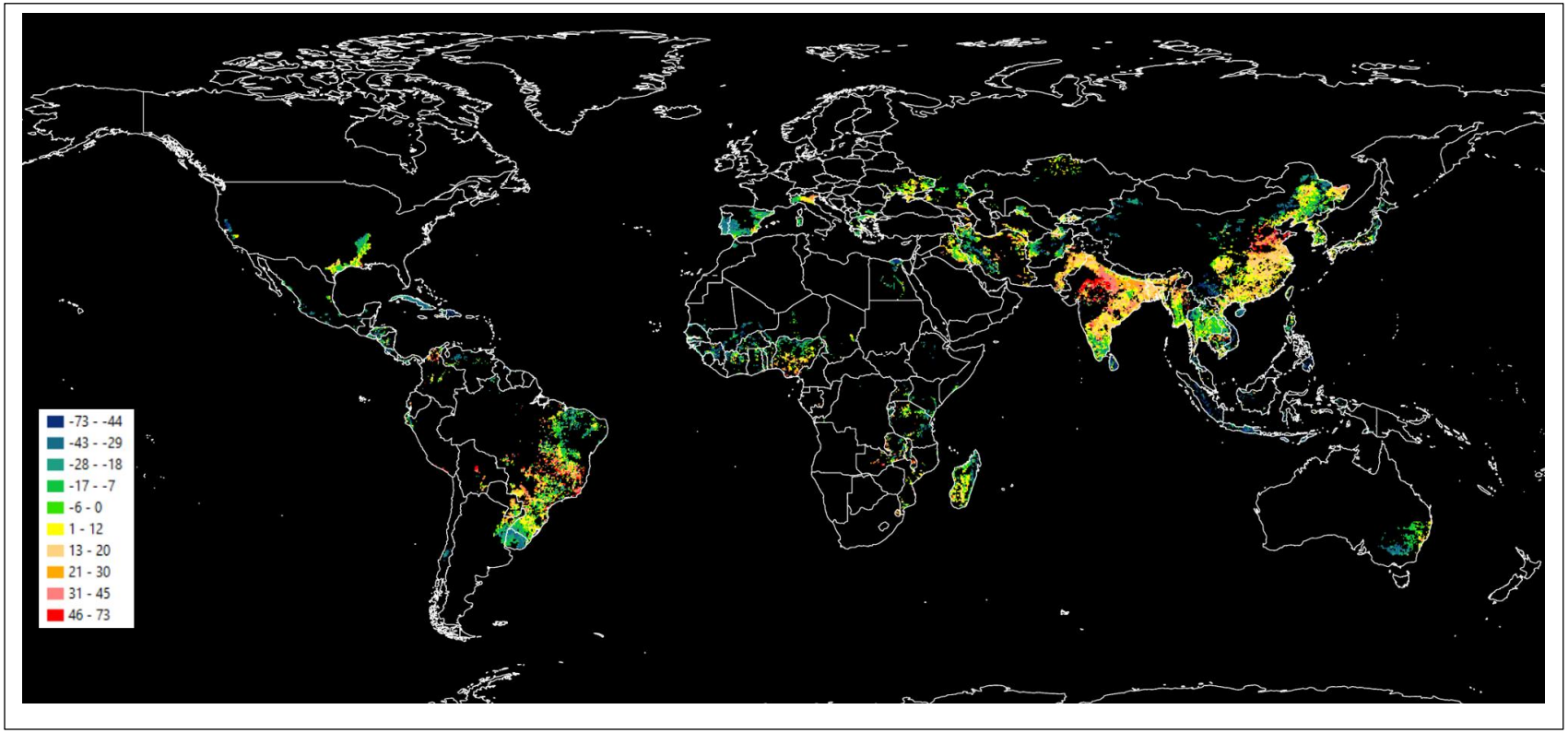

Table 4: Local S5P methane anomalies: Outlier states/provinces

ISO3	Country	State/Province	Mean Residual
BOL	Bolivia	Cochabamba	45.8
IND	India	Rajasthan	42.4
BRA	Brazil	Rio de Janeiro	41.8
CHN	China	Shandong	38.0
BRA	Brazil	Espírito Santo	35.6
IND	India	Madhya Pradesh	34.3
CHN	China	Henan	32.6
MMR	Myanmar	Kachin	31.5
NGA	Nigeria	Cross River	29.4
IND	India	Uttar Pradesh	27.1
ITA	Italy	Veneto	25.6
PAK	Pakistan	N.W.F.P.	25.4
NGA	Nigeria	Edo	25.3
IND	India	Gujarat	25.3
PRY	Paraguay	Misiones	24.7
AZE	Azerbaijan	Aran	24.5
IND	India	Bihar	24.3
MMR	Myanmar	Shan	23.3
IND	India	Maharashtra	23.3
BOL	Bolivia	Chuquisaca	23.0
PRT	Portugal	Santarém	-33.5
URY	Uruguay	Lavalleja	-33.8
MLI	Mali	Timbuktu	-33.9
JPN	Japan	Fukushima	-34.0
GIN	Guinea	Kankan	-34.8
CUB	Cuba	Camagüey	-35.6
PRT	Portugal	Portalegre	-35.7
CUB	Cuba	Sancti Spíritus	-35.7
URY	Uruguay	Artigas	-36.7
IDN	Indonesia	Sulawesi Selatan	-37.9
EGY	Egypt, Arab Rep.	Al Buhayrah	-38.0
CHN	China	Yunnan	-38.2
VEN	Venezuela, RB	Portuguesa	-38.3
IDN	Indonesia	Riau	-39.1
IDN	Indonesia	Jawa Tengah	-41.1
IDN	Indonesia	Jawa Timur	-41.9
IDN	Indonesia	Sumatera Utara	-42.4
MLI	Mali	Mopti	-42.9
IDN	Indonesia	Sumatera Selatan	-48.5
IDN	Indonesia	Bengkulu	-51.7

8. The Spatial Distribution of S5P CH4 Intensities for Irrigated Rice Production

Local S5P CH4 anomalies also provide new information about the spatial distribution of CH4 intensity for irrigated rice production, which we index as the difference between the CH4 percentile and the rice production percentile from IFPRI (2019). This can be interpreted as an index of the methane produced per unit of food value. Figure 8 displays the spatial distribution, which features an unbalanced incidence of positive and negative outlier clusters (with high and low methane intensities, respectively). Large clusters of the former are concentrated almost entirely in northern Pakistan and northern India. On the other hand, significant clusters of the latter are identifiable in southeastern Australia, southwestern and far western China, the Nile Delta and river valley, northeast Tanzania, northern Côte d'Ivoire, southwestern Spain, Uruguay, western coastal Peru, western Honduras and California.

Table 5 provides a summary view for states/provinces that have more than 10 observations. The table displays top-20 positive and negative outliers in descending order. Among the countries with positive outliers, Brazil and Nigeria are represented by 4 areas; three countries by 2 areas (India, Myanmar, Bolivia); and six countries by 1 (China, Cambodia, Pakistan, the Islamic Republic of Iran, Zambia, Paraguay). Among countries with negative outliers, Indonesia leads with 7 areas, followed by Mali (4), Uruguay (3), Thailand (2) and four countries with 1 area (China, Egypt, Senegal and the República Bolivariana de Venezuela). In summary, Brazil and Nigeria dominate the positive outlier countries and Indonesia, Mali and Uruguay dominate among negative outliers. Full results are available from the authors on request.

Figure 8: S5P CH4 intensities of rice production

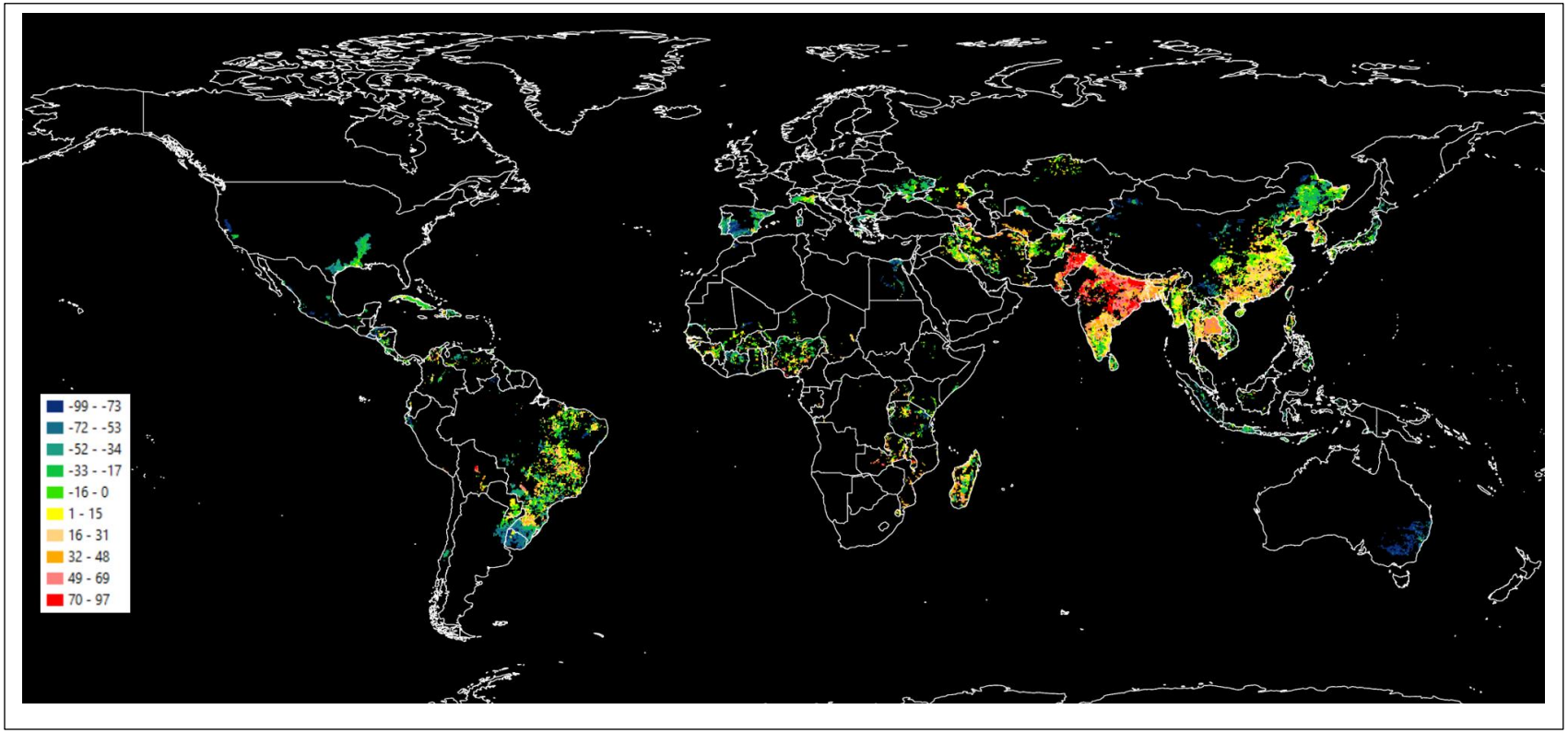

Table 5: S5P CH4 intensity indices: Outlier states/provinces

ISO3	Country	State/Province	Mean Index
BOL	Bolivia	Cochabamba	72.2
NGA	Nigeria	Cross River	*58.8*
BRA	Brazil	Espírito Santo	*53.1*
MMR	Myanmar	Tanintharyi	*52.2*
NGA	Nigeria	Edo	*51.5*
BRA	Brazil	Rio de Janeiro	*50.8*
CHN	China	Shandong	*46.0*
IND	India	Rajasthan	*43.9*
BOL	Bolivia	Chuquisaca	*43.8*
MMR	Myanmar	Kachin	*42.7*
IND	India	Madhya Pradesh	*41.4*
BRA	Brazil	Goiás	*41.2*
NGA	Nigeria	Benue	*40.9*
KHM	Cambodia	Preah Vihéar	*39.1*
IRN	Iran, Islamic Rep.	Yazd	*38.9*
PRY	Paraguay	San Pedro	*38.6*
PAK	Pakistan	N.W.F.P.	*38.2*
ZMB	Zambia	Lusaka	*38.1*
NGA	Nigeria	Nassarawa	*37.6*
BRA	Brazil	Mato Grosso	*37.0*
URY	Uruguay	Lavalleja	*-39.8*
URY	Uruguay	Cerro Largo	*-39.9*
MLI	Mali	Ségou	*-42.3*
THA	Thailand	Lampang	*-43.4*
CHN	China	Yunnan	*-43.7*
IDN	Indonesia	Sumatera Utara	*-44.0*
URY	Uruguay	Artigas	*-44.1*
SEN	Senegal	Saint-Louis	*-46.5*
MLI	Mali	Mopti	*-46.6*
VEN	Venezuela, RB	Portuguesa	*-47.2*
IDN	Indonesia	Sulawesi Selatan	*-47.9*
MLI	Mali	Koulikoro	*-48.4*
IDN	Indonesia	Jawa Barat	*-51.0*
IDN	Indonesia	Bengkulu	*-52.9*
THA	Thailand	Chiang Mai	*-53.0*
IDN	Indonesia	Sumatera Selatan	*-53.1*
EGY	Egypt, Arab Rep.	Al Buhayrah	*-55.5*
MLI	Mali	Timbuktu	*-60.3*
IDN	Indonesia	Jawa Tengah	*-60.5*
IDN	Indonesia	Jawa Timur	*-62.5*

9. Summary and Conclusions

The Global Methane Pledge joins 122 countries in a collective effort to reduce global methane emissions at least 30 percent from 2020 levels by 2030. This paper is intended to support Pledge participants in a two-part exercise. First, it introduces a new World Bank database that reports monthly atmospheric methane (CH4) concentrations for the terrestrial globe in a spatial grid with a resolution of 25 km. Monthly means are calculated for "local anomalies" in bias-corrected XCH4 data from the European Space Agency's Sentinel-5P (TROPOMI) satellite platform. The new database computes monthly mean values from daily time-stamped observations that have been pre-filtered for global, seasonal and latitudinal background effects. We term these "local anomalies" because they register the local emissions component of the data. Recent global research (Sha et al. 2021) has shown that the Sentinel-5P methane measures align closely with measures taken by ground stations in TCCON (the Total Carbon Column Observing Network). The database will be maintained online by the Development Data Hub of the World Bank's Development Economics Vice Presidency.

The new database is intended to assist Pledge participants in reducing methane emissions from energy, agricultural and waste subsectors whose spatial distributions are highly non-uniform across and within countries. At present, priority areas for emissions reduction are identified with spatially-formatted "bottom-up" estimates provided by national or global emissions inventories such as the Emissions Database for Global Atmospheric Research (EDGAR). These inventories combine sectoral activity data with broadly calibrated emissions factors. Using spatial inventories like EDGAR, policy analysts can identify emissions-intensive areas, trace the emissions to specific subsectors, and perform benefit-cost assessments of alternative technologies for emissions reduction.

The second part of the paper explores the potential contribution of Sentinel-5P data to the selection of priority areas. The value added of satellite-based methane observations can only be judged after a round of comparative empirical work. In this paper, we contribute with a pilot study of CH4 emissions from irrigated rice production, which accounts for about 10% of agricultural CH4 emissions. Rice production in flooded fields produces methane because oxygen does not penetrate the soil when it is blocked by water. This promotes the growth of methane-producing bacteria. A variety of techniques can shorten the period of water blockage, including a single field drainage in the mid-season; alternate wetting and drying (AWD), dry seeding instead of transplanting rice into flooded fields, and "aerobic" systems that grow rice in well-drained soil. Our study aims to use the Sentinel-5P (S5P) database to learn more about local variations in methane emissions created by differences in water use and the configuration of rice fields.

We draw monthly CH4 anomaly observations from the database for areas and seasons identified by spatially-referenced data on irrigated rice production from IFPRI and seasonal production timing from RiceAtlas. We compute mean values by grid cell for the period 2020-2022 and explore their relationship with three spatially-referenced data sets that are resampled to match the 25-km global grid: (1) IFPRI estimates of irrigated rice field extents; (2) estimates of agricultural methane emissions from EDGAR, a "bottom-up" inventory that combines detailed

sectoral activity estimates with emissions factors that vary by region; and (3) IFPRI estimates of rice production, which we combine with our CH4 anomaly observations to index relative methane intensities (emissions per unit of output) for different areas.

Regression analysis reveals a highly significant relationship between IFPRI irrigated field extents and local SP5 CH4 anomalies. We map expected values from the regression results, as well as regression residuals that identify areas where the CH4 anomalies identify methane concentrations that are higher and lower than expectations from field extents alone. For comparison, we also perform a regression analysis of the relationship between methane emissions estimated by EDGAR and irrigated field extents. As expected, we find a closer "fit" for EDGAR emissions because their "bottom-up" computation actually incorporates field extent. In a follow-on exercise, we regress local CH4 anomalies on field extent and EDGAR emissions and use the residuals to identify outlier areas with unexpectedly high or low emissions. These residuals represent the "value added" of the S5P data, because they identify local methane emissions variations that are not captured by IFPRI field extent or EDGAR estimates. The regression residuals identify a large number of positive and negative outlier clusters in all regions. We map these results and summarize them by identifying the states and provinces within countries that have the largest positive and negative outlier values.

Finally, we compute a spatial measure of methane intensity that indexes CH4 emissions per unit of output. This information is particularly interesting from a development perspective, since it incorporates the food value of rice production as well as the associated methane emissions. We find particularly high and low methane intensities among Indian states and Indonesian provinces, respectively, along with smaller clusters of positive and negative outlier states/provinces in Asia and other global regions.

In summary, this first application of the new World Bank database suggests that CH4 atmospheric concentration measures from the ESA's Sentinel-5P system can provide useful new information for identifying and assessing local variations in methane emissions from irrigated rice production. While more ground-truthing would undoubtedly be useful, we believe that recent research has already established the accuracy of space-based CH4 measures. For irrigated rice production, future survey research could shed more light on the local sources of variation in measured emissions. This could in turn support incentive-based programs that use the World Bank database to track, verify and reward adoption of methane-reducing techniques. If this approach proves valuable for irrigated rice production, we believe that it can work for other methane sources as well.

References

Adhya, T. K. et al. 2014. “Wetting and Drying: Reducing Greenhouse Gas Emissions and Saving Water from Rice Production.” Working Paper, Installment 8 of Creating a Sustainable Food Future. Washington, DC: World Resources Institute.

Ciais, P., et al. 2013. Carbon and Other Biogeochemical Cycles, in Climate Change 2013: The Physical Science Basis, Contribution of Working Group I to the Fifth Assessment Report of the Intergovernmental Panel on Climate Change, edited by: T. Stocker et al. Cambridge University Press, Cambridge, UK, New York, NY.

Crippa, M., E. Solazzo, G. Huang, D. Guizzardi, et al. 2020. High resolution temporal profiles in the Emissions Database for Global Atmospheric Research. Sci Data 7: 121.

Dasgupta, S., S. Lall and D. Wheeler. 2022a. Subways and CO2 Emissions: A Global Analysis with Satellite Data (under review for publication).

Dasgupta, S., S. Lall and D. Wheeler. 2022b. Scalable Tracking of CO2 Emissions: A Global Analysis with Satellite Data (under review for publication).

Devkota, K. et al. 2019. Economic and environmental indicators of sustainable rice cultivation: A comparison across intensive irrigated rice cropping systems in six Asian countries. Ecological Indicators 105: 199–214.

EDGAR (Emissions Database for Global Atmospheric Research). 2022. Global Greenhouse Gas Emissions - EDGAR v6.0. Sector-Specific Gridmaps: N2O - IPCC 4C+4D - Agricultural soils. https://edgar.jrc.ec.europa.eu/gallery?release=v60ghg&substance=N2O&sector=AGS

Etminan, M., G. Myhre, E. Highwood and K. Shine. 2016. Radiative forcing of carbon dioxide, methane, and nitrous oxide: A significant revision of the methane radiative forcing. Geophysical Research Letters 43: 12614–12623.

FAO (Food and Agriculture Organization of the United Nations). 2014. FAOSTAT. Rome: FAO. http://faostat.fao.org

Fischer, T., D. Byerlee, and G. Edmeades. 2014. “Crop Yields and Global Food Security: Will Yield Increases Continue to Feed the World?” ACIAR Monograph No. 58. Canberra, Australia: Australian Center for International Agricultural Research.

GADM. 2022. Maps for the administrative areas of all countries. https://gadm.org/data.html

Hakkarainen, J., I. Ialongo, S. Maksyutov and D. Crisp. 2019. Analysis of Four Years of Global XCO2 Anomalies as Seen by Orbiting Carbon Observatory-2. Remote Sensing 11, no. 7: 850.

IFPRI (International Food Policy Research Institute). 2019. “Global Spatially-Disaggregated Crop Production Statistics Data for 2010 Version 2.0”, https://doi.org/10.7910/DVN/PRFF8V, Harvard Dataverse, V4.

IRRI (International Rice Research Institute). 2022. How to Manage Water. Rice Knowledge Bank. Available online at http://www.knowledgebank.irri.org/step-by-step-production/growth/water-management.

Laborte, A. et al. 2017. RiceAtlas, a spatial database of global rice calendars and production. Nature Scientific Data 4:170074.

Labzovskii, L., S. Jeong and N. Parazoo. 2019. Working towards confident spaceborne monitoring of carbon emissions from cities using Orbiting Carbon Observatory-2. Remote Sens. Environ. 233: 111359.

Myhre, G. et al. 2013. Anthropogenic and Natural Radiative Forcing, in Climate Change 2013: The Physical Science Basis, Contribution of Working Group I to the Fifth Assessment Report of the Intergovernmental Panel on Climate Change, edited by: T. Stocker et al. Cambridge University Press, Cambridge, UK, New York, NY, USA.

Nassar, R., J. Mastrogiacomo, W. Bateman-Hemphill, et al. 2021. Advances in quantifying power plant CO2 emissions with OCO-2. Remote Sensing of Environment. 264: 112579.

Nguyen, V. et al. 2022. An assessment of irrigated rice cultivation with different crop establishment practices in Vietnam. Nature Scientific Reports 12: 401.

Pan, G., X. Yuan and M. Jieqi. 2021. The potential of CO2 satellite monitoring for climate governance: A review. Journal of Environmental Management, 277: 111423.

Prather, M., C. Holmes and J. Hsu. 2012. Reactive greenhouse gas scenarios: Systematic exploration of uncertainties and the role of atmospheric chemistry. Geophysical Research Letters 39: L09803.

Reuters. 2018. Global temperatures on track for 3-5 degree rise by 2100: U.N. https://www.reuters.com/article/us-climate-change-un/global-temperatures-on-track-for-3-5-degree-rise-by-2100-u-n-idUKKCN1NY186?edition-redirect=uk

Saunois, M. et al. 2020. The Global Methane Budget 2000–2017. Earth System Science Data 12: 1561–1623.

Sha, M., et al. 2021. Validation of methane and carbon monoxide from Sentinel-5 Precursor using TCCON and NDACC-IRWG stations, Atmospheric Measurement Techniques, 14: 6249–6304.

Shindell, D. et al. 2012. Simultaneously Mitigating Near-Term Climate Change and Improving Human Health and Food Security. Science 335: 183–189.

Solazzo, E., M. Crippa, D. Guizzardi, M. Muntean, M. Choulga and G. Janssens-Maenhout. 2021. Uncertainties in the Emissions Database for Global Atmospheric Research (EDGAR) emission inventory of greenhouse gases. Atmospheric Chemistry and Physics, 21: 5655–5683.

Steffen, W., J. Rockström and K. Richardson. 2018. Trajectories of the Earth System in the Anthropocene. PNAS 115(33): 8252-8259.

Stuart, A. et al. 2018. On-farm assessment of different rice crop management practices in the Mekong Delta, Vietnam, using sustainability performance indicators. Field Crops Research 229: 103–114.

Weir, B., D. Crisp, C. O'Dell, et al. 2021. Regional impacts of COVID-19 on carbon dioxide detected worldwide from space. Science Advances, 7(45).

World Bank. 2012. Turn Down the Heat ~ Why a 4°C warmer world must be avoided. World Bank: Washington, D.C.

Wu, D., J. Lin, T. Oda and E. Kort. 2020. Space-based quantification of per capita CO2 emissions from cities. Environmental Research Letters, 15: 035004.

Yu, Q., et al. 2020. A cultivated planet in 2010 – Part 2: The global gridded agricultural-production maps, Earth System Science Data 12: 3545–3572.